Shahid Bahonar University of Kerman

Biomechanism and Bioenergy Research

Online ISSN: 2821-1855
Homepage: https://bbr.uk.ac.ir

Iranian Society of Agricultural Machinery Engineering and Mechanization

Design, Manufacture and Evaluation of Oat De-Husking Machine

Kaumars Merikhi[1], Hekmat Rabbani[2]✉, Sohbat Bahraminejad[3]

[1] Mechanical Engineering of Biosystems Department, Tehran University, Tehran, Iran.
[2] Mechanical Engineering of Biosystems Department, Razi University, Kermanshah, Iran.
[3] Plant Genetics and Production Department, Razi University, Kermanshah, Iran.

✉ Corresponding author: hrabbani2010@gmail.com

ARTICLE INFO

Article type:

Research Article

Article history:

Received 11 October 2024

Received in revised form 28 November 2024

Accepted 11 December 2024

Available Online 31 December 2024

Keywords:

Oat, Husking, Design, Manufacturing, Separation

ABSTRACT

Peeling is an essential step in oat processing. In the operation of peeling oats with peeling machines, a percentage of oats will break and cause quality waste in the product. In this study for the first time, the skin-separating mechanism was created by the contact of two surfaces of the conveyor belt, where the belt passes by the seeds at a higher speed. The upper and lower belts are flat types with 2 mm space, based on the average value of the width of six varieties of oats. The lower belt has a lower speed than the upper belt, the seeds fall on it and move forward. While the upper belt has a higher speed, it causes the rotational movement of the seed by moving on the seeds, and while the seed is between the two belts, it is under pressure, and due to this pressure and rotational movement, the seed skin is broken and separated. To prevent the lower belt from bending, a tray is installed under the lower belt. The amount of dehulled grain is calculated based on the speed of the lower belt. According to the calculations, having a reliability factor of 2, an electric motor of 4 horsepower at 1500 rpm has been selected. The upper speed of the belt is 31.4 m/min and the outlet opening of the tank is 0.003 m^2. The amount of peeled oats is 486 kg per hour. In the evaluation of the peeling machine, 76% of Euro varieties was obtained.

Cite this article: Merikhi, K., Rabbani, H., & Bahraminejad, S (2024). Design, Manufacture and Evaluation of Oat De-Husking Machine. *Biomechanism and Bioenergy Research*, 3(2), 164-174. https://doi.org/10.22103/bbr.2024.24358.1101

Publisher: Shahid Bahonar University of Kerman
DOI: https://doi.org/10.22103/bbr.2024.24358.1101

INTRODUCTION

Today, with the advancement of science and knowledge, we are constantly witnessing an increase in the diversity and quantity of food available to humans. With the growth of science, humans have been able to bring more wild plants and animals under their control. One of the products that has been cultivated in recent years is a plant called oats. Oats are grown in Northern European countries, and for the past few years, research centers in Iran have been cultivating oats as a research crop.

Oats, or Avena Sativa, is a newer crop compared to plants like wheat and barley, with its origin in Europe, China, and Western Asia, where it was first cultivated around 522 BCE. This plant can yield better results under relatively poor soil conditions or when grown in unfavorable environments, which is one of the factors contributing to its popularity. Especially after the development of resistant varieties in 1542, oat production worldwide has increased. The production of the top four countries—Russia, Canada, Poland, and Australia—along with global production, stands at 5, 3.8, 1.2, 1.1, and 24 million tons, respectively (Doehlert, 2002). Oats are highly valued for their high nutritional content, including significant amounts of protein, fat, and beneficial compounds like beta-glucan, as well as a favorable amino acid composition (Mirmoghtadaie et al., 2013; Yang et al., 2023).

In another study, the design, construction, and evaluation of a pistachio dehulling machine were addressed. In this method, pistachios with green skins are initially fed into the machine from the upper part of the hopper, after which the bottom of the hopper and the walls move in opposite directions. The bottom of the hopper has a rough surface, forming a mixture shape. This results in a frictional force being applied to the pistachio each time it comes into contact with the bottom of the hopper. The rotation of the hopper walls in the opposite direction of the bottom creates a lateral force on the pistachio. After a certain period of rotation, the movement of the hopper walls is stopped, and while the bottom continues to rotate, pressurized water is injected via a nozzle to wash off the skin from the pistachios. After washing, the walls of the hopper rotate in the same direction as the bottom for drying. In the final stage, the hopper walls are stopped, and by rotating the bottom and opening a side hatch of the hopper, the dehulled pistachios are discharged (Khodabakhshian et al., 2010).

A peanut dehulling machine was designed using a metal cylinder with a rubber-coated, grooved surface (impacting element) rotates against a metal mesh (counter-impacting element). The peanut pods are fed into the space between the impacting and counter-impacting elements via a hopper, and the rotation of the impacting element against the counter-impacting element separates the skin from the pod. The mixture of skin and kernels passes through the counter-impacting element and falls into a sloped tray. In this design, airflow helps to separate the skin from the kernels. The inclined tray allows the kernels, which have a higher specific weight than the skin, to slide downward and exit from one side of the tray. The skin is blown out from the other side of the tray by the airflow, effectively separating the skin from the kernels (Rostami, 2008).

Based on these information and previous research, as well as the increasing acreage dedicated to oat cultivation and the lack of appropriate oat de-husking machine, there is a need in the agricultural industry for an oat de-husking machine. The objective of this research was to design and construct an oat de-husking machine using the abrasive mechanism developed by two conveyor belts.

MATERIALS AND METHODS

The main design is based on the movement of two conveyor belts operating in opposite directions at different speeds. In this design, the lower conveyor belt is longer than the upper one, and the two belts overlap. The product is placed on the lower belt, which moves it forward, guiding it between the two belts. Meanwhile, the upper belt, which moves faster, pushes the grains forward. As the grains move, they experience a rolling motion and slight pressure. These movements exert forces on the grains, causing the husk to crack and separate from the kernel. The husk of the oats is slightly detached from the kernel, and this distance, combined with the rotation of the

belts, causes the husk to bend and slide, leading to its breakage (Figure 1).

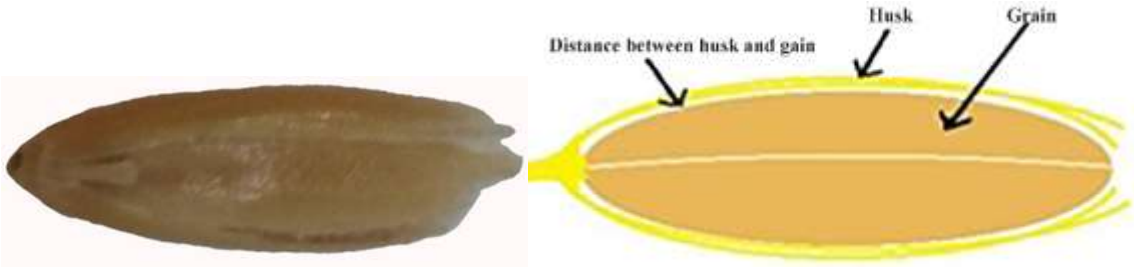

Figure 1. Schematic of oat grain (right) main view of oat (left).

Engine selection

Every machine requires a power source, and one of these sources is the electric motor. Due to the simplicity of using electric motors, they are commonly found in most machines around us today. Each electric motor has a specific power at a given speed, so selecting the appropriate motor has a significant impact on the machine's lifespan and efficiency. In a designed machine, most of the energy is consumed to overcome the friction in the oat dehulling belts and to set them in motion (Asli-Ardeh et al., 2022).

To calculate the required power for moving the flat belts, we need to consider the power needed per 100 mm width of the belt. As mentioned, for every 100 mm of belt width, 0.2 horsepower is required, and the belts have an efficiency of 70% to 96% (Babeski et al., 2023). Therefore, assuming 90% efficiency, the required power for the upper belt width of 30 cm and the lower belt width of 50 cm is equal to:

Because there are two series of belts before the power reaches both flat belts. As a result:

$$P = \frac{(500+300)}{100} \times 0.2 \times \frac{100}{90} \times \frac{100}{90} = 1.97hp \simeq 2hp \quad (1)$$

Therefore, considering a safety factor of 2, a 4-horsepower, 1500 RPM, three-phase, single-speed industrial electric motor with standard efficiency (IE1), manufactured by Motojen, has been selected.

Power transmission system

Motors generate power, and this power is used to overcome friction and set the machine components in motion. The power transmission system consists of various parts that deliver power from the motor to the main sections of the machine. In the power transmission system, both speed and torque can be adjusted during power transfer. The designed machine includes three V-shaped belts, with the motor belt being of the double-sided type. The stages of power transmission are as follows:

1. Power transmission via a hexagonal belt from the motor to the lower conveyor belt.
2. Power transmission via a hexagonal belt from the motor to the upper conveyor belt.

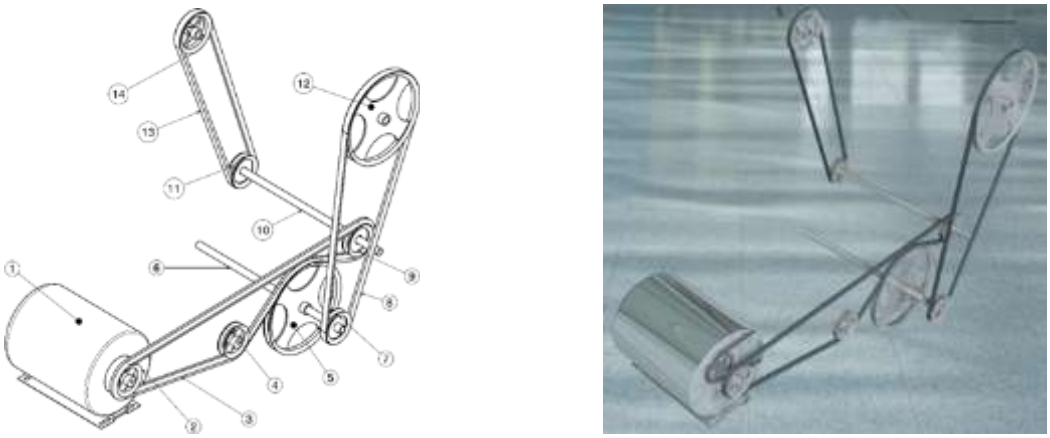

Figure 2. Power transmission system; 1- motor, 2- engine pulley (diameter in 3/5), 3- hexagonal belt (80 AA), 4- hexagonal belt adjustment pulley (moving pulley) (diameter in 3/5), 5, 12- pulley Big (diameter 11 in), 6, 10- axis, 7, 9, 11- small pulley (diameter 3/5 in), 8- power transmission belt to the lower conveyor belt (71 A), 13- power transmission belt to the belt Upper conveyor (58 A), 14-medium pulley (diameter 5 in).

Choosing the type and section of the belt

Considering the impact of sectional dimensions on the load-bearing capacity of the belts, the first step in designing belt-driven systems is selecting the belt's cross-section. The cross-section of the belt is chosen using standard charts, based on the power that is to be transmitted by a single row of belts and the rotational speed of the smaller pulley (motor pulley).

The appropriate cross-section is obtained from the chart based on the transmitted power in horsepower (hp) and the rotational speed of the smaller pulley in revolutions per minute (RPM). If the transmitted power is so high that none of the belt cross-sections are suitable, or if for any reason a smaller cross-section belt is preferred, then multiple belts should be used in parallel. In this case, the transmitted power should be divided by the number of belts, and the appropriate cross-section should be selected from the chart accordingly (Amiss et al., 2004).

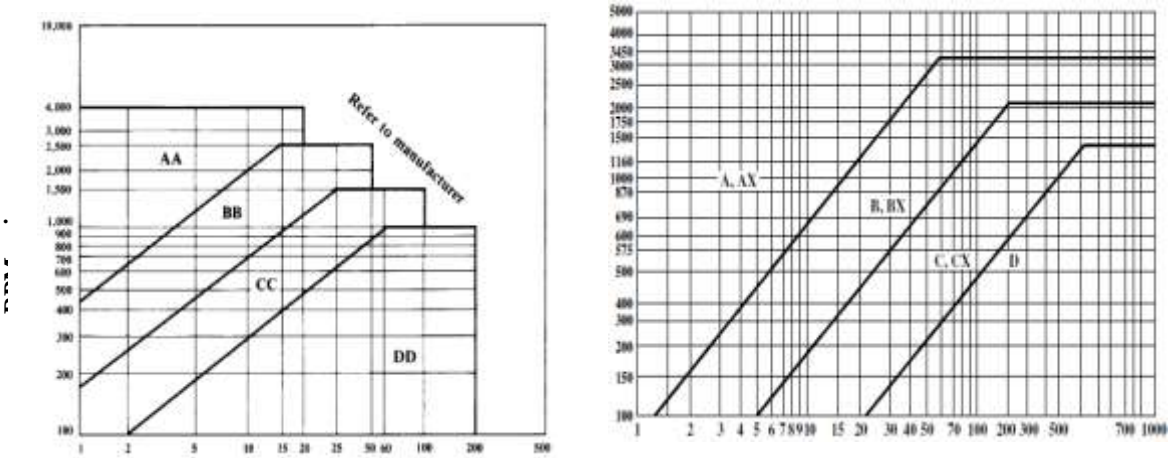

Horsepower design
(Horsepower in choosing the X factor)

Figure 3. Choosing the cross-section of one and two-way V-shaped belts (Amiss et al., 2004).

As shown in Figure 2, a hexagonal belt is used in the power transmission system in such a way that it transmits power to two subsequent pulleys. Therefore:

By selecting a motor with 4 horsepower and 1500 RPM, and considering the 4 horsepower in the horizontal chart and 1500 RPM (as shown in Figure 3), the belt cross-section type is located in section AA. Therefore, by choosing a belt with an AA cross-section, the force is transmitted to the subsequent pulleys.

Based on the calculations, it was found that for the lower flat belt, 1.23 horsepower is required, and for the upper flat belt, 0.74 horsepower is needed. The hexagonal belt transmits this power to both power transfer paths. However, in the further sections of the power transmission path, V-belts with standard ANSI/RMA IP-20 specifications are used. Looking at Figure 3, it is observed that the cross-section of the belt in these sections is of type A. Therefore, the type of belt used in this stage is a belt with an A cross-section.

Calculation of Pulley Pitch Diameter and Determining the Pulley Size

The lifespan of a belt is directly related to the diameter of the pulley, and as the diameter of the pulley decreases, the lifespan of the belt also decreases. Therefore, the minimum diameter of the small pulley cannot be chosen smaller than a certain limit. The minimum reference diameter for the pulley for different belt sections can be obtained from the following relationship (Amiss et al., 2004; Avallone et al., 2006).

$$d_p = d + 2h_d - 2a_p \quad (2)$$

d_p: diameter of the pulley pitch (in). d: base diameter (in). h_d, and a_p: parameters of pulley diameter (in).

Therefore, based on the tables and the above formula, considering the cross-section AA, the minimum diameter of the small pulley is chosen to be 3.5 inches. The minimum pulley used in this design for V-belts is set at 3.5 inches. Consequently, the diameters of pulleys number 7, 11, 12, and 14 are selected as 3.5, 3.5, 11, and 5 inches, respectively.

Determining the standard length of the belt

The appropriate ways to select the length of hexagonal belts is by measuring the belt path length. On the belts, there are a series of numbers, one of which is the belt number. This number is slightly different from the effective length of the belt.

Table 1. The lengths that should be added to the circumference of the two-sided V-shaped belt to obtain the circumference in inches (Amiss et al., 2004).

Cross-section of the belt	AA	BB	CC	DD
The amount of increase in the internal environment	2.1	2.9	4.1	5.2

The length of V-shaped belts is calculated using the following formulas (Amiss et al., 2004).

$$\theta_d = \pi - 2\sin^{-1}\frac{D_P - d_P}{2C} \quad (3)$$

$$\theta_D = \pi + 2sin^{-1}\frac{D_P - d_P}{2C}$$

$$L = [4C^2 - (D_P - d_P)^2]^{1/2} + \frac{1}{2}(D_P\theta_D - d_P\theta_d) \quad (4)$$

In the above relations: L: total length of belt (in). C: center-to-center distance of two pulleys (in). D_p: Pitch diameter of the large pulley (in). d_p: Pitch diameter of the small pulley (in). θ_D: the contact angle of the belt with the large pulley (rad). θ_d: the contact angle of the belt with the small pulley (rad).

Table 2. Lengths to be added to the U.S. standard V-belt inner circumference to obtain the pitch circumference in inches.

Cross-section of the belt	A	B	C	D	E
The amount of increase in the internal environment	1.3	1.8	2.9	3.3	4.5

Given that obtaining the standard belt length changes the center distance between the two pulleys, therefore the new distance is calculated. To calculate the new distance, a series of

coefficients and formulas are used (Amiss et al., 2004; Budynas & Nisbett, 2011).

Center distance correction coefficient (K):

$$K = 4L_S - 2\pi(D_P + d_d) \quad (5)$$

Calculating the distance between the centers (C_m):

$$C_m = \frac{K + \sqrt{K^2 - 32(D_P + d_d)^2}}{16} \quad (6)$$

The resulting standard length for belt AA is number 80, belt number 8 is also determined by measuring the inner circumference length of the belt which was 73.177 inches, and with a reduction of 1.3, the belt number is 71 A. The standard length of belt number 13 is also 58 A.

Speed calculations in pulleys

In power transmission paths with pulleys, the speed of each pulley is measured based on its pitch diameter and the speed of each pulley.

$$S = \frac{d_p \times s}{D_p} \quad (7)$$

S: Large pulley speed (rpm). D_p: diameter of large pulley (in). s: engine pulley speed (rpm). d_p: diameter of small pulley (rpm).

Speed calculations showed that the speeds in pulleys number 5, 9, 12, and 14 are 500, 1500, 167, and 1071 RPM (revolutions per minute) respectively.

Belt speed calculations

The belt speed is determined by the motor's RPM (revolutions per minute) or driving pulley speed concerning the pulley diameter (Amiss et al., 2004).

Hexagonal belt speed calculation:

$$r = \frac{s}{1000} \quad (8)$$

$$S = \frac{rd_p}{3.820} \quad (9)$$

r: Angular speed of the motor pulley (drive pulley), (rpm/1000). s: pulley speed (rpm). S: belt speed (fpm/1000). d: pulley diameter (in).

V-belt speed calculation (Budynas & Nisbett, 2011):

$$V = \frac{\pi dn}{12} \quad (10)$$

V: belt speed (ft/min). d: Diameter of the 7-pulley pitch (in). n: pulley speed (rpm).

Calculation of stresses applied to each belt

When power is transferred from one pulley to the next via a belt, we observe a series of stresses in the belts. These stresses vary based on the pulley diameter and the amount of power being transferred. Using this information, we calculate the maximum stress tolerance of each belt and determine the number of belts required, which we will examine here.

Stress in hexagonal belt

The calculation is carried out using the following formulas (Amiss et al., 2004):

$$T_e = \frac{33P_d}{S} \quad (11)$$

T_e: effective pulley stress (lbf). P_d: transfer load with pulley (hp).

$$T_T = T_e[\frac{R}{(R-1)}] \quad (12)$$

T_T: Pulley tight side belt stress (lbf).

$\frac{R}{(R-1)}$: Minimum stress ratio factor.

$$T_S = T_{T-}T_e \quad (13)$$

T_S: Belt stress on the loose side of the pulley (lbf).

Calculation of the allowable stress on the stiff side of the double-sided belt AA (Amiss et al., 2004):

$$T_r = 118.5 - \frac{318.2}{d_p} - 0.8380S^2 - 25.76logS \quad (14)$$

T_r: allowable stress on the rigid side (lbf). dp: diameter of the pulley pitch (in). S: belt speed (fpm/1000).

The stress resulting from the motor pulley is 27, therefore, more than one row of belts must be used.

The stress in the V-shaped belt

The V-shaped belts also experience stress on both sides of the pulley, with the stress differing on each side. Utilizing the formulas below, this stress can be calculated (Budynas & Nisbett, 2011).

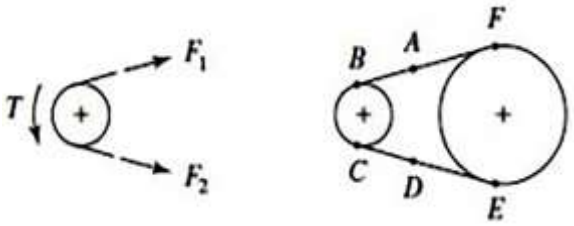

Figure 4. Creating stress in the belt

$$\exp(0.5123\theta_d) \quad (15)$$

$\exp(0.5123\theta_d)$: stress coefficients. θ_d: contact angle of the belt with the small pulley (rad).

$$F_c = K_c(\frac{V}{1000})^2 \quad (16)$$

F_c: unit centrifugal force (lbf). K_c: belt coefficients. V: unit belt speed (ft/min).

$$\Delta F = \frac{63025\frac{H_d}{N_b}}{n\frac{d}{2}} \quad (17)$$

F_Δ: the difference in stress between the pulley sides (lbf). H_d: input power to drive motor (h_p). N_b: Number of belts. n: number of engine revolutions (rpm). d: Diameter of the pulley pitch (in).

$$F_1 = F_c + \frac{\Delta F exp(0.5123\theta_d)}{exp(0.5123\theta_d) - 1} \quad (18)$$

F_1: force on the cross-section of the rigid side belt (lbf). θ_d: contact angle of the belt with the small pulley (rad).

$$F_2 = F_1 - \Delta F \quad (19)$$

F_2: force acting on the cross-section of the loose side belt (lbf).

Belt number 8 experiences a force of 12.7 (lbf) acting on its section, while belt number 13 exhibits a stress of 5.53(lbf).

Calculation of transmission power with belts

One method of power transmission involves the use of belts, which can connect driving and driven shafts even over relatively considerable distances. This mode of power transfer varies depending on the type of belt employed.

Power transmission utilizing hexagonal belts and multiple rows of belts.

In hexagonal belts, the required power is assumed, and calculations for transmission are subsequently performed. Ultimately, the transmitted power is determined by evaluating the generated stress in the belt, comparing it with the permissible stress ratio, and taking into account both the assumed power and the adjusted power (Amiss et al., 2004).

Determining the correction factor for length (K_f):

$$\frac{L_e}{n} \quad (20)$$

L_e: effective belt length (in). n: the number of pulleys placed in the hexagonal belt path.

Calculating the required number of belt rows:

$$N_b = \frac{T_T}{T_t K_f} \quad (21)$$

N_b: number of belt rows. T_r: allowable stress on the rigid side (lbf). T_T: Pulley tight side belt Stress (lbf). K_f: Length correction coefficient.

The number of hexagonal belt rows required for this device is three.

Power transmission utilizing type A V-belts and the number of belt rows:

The amount of power transmitted through each section of the belt is determined by a specific formula corresponding to the type of belt. In the case of Type V belts, the following calculations are utilized (Amiss et al., 2004; Budynas & Nisbett, 2011).

$$r = \frac{S}{1000} \tag{22}$$

r: angular speed of the motor pulley (drive pulley), (rpm/1000). S: pulley speed (rpm).

The speed ratio and speed correction factor (K_{SR}) (Amiss et al., 2004).

$$\frac{S_{d_p}}{S_{D_p}} \tag{23}$$

S_{dp}: Angular speed of smaller spool (rpm). S_{Dp}: Larger angular speed (rpm).

Calculation of power transmission using type A V-belts (Budynas & Nisbett, 2011).

$$HP = d_p r \left[1.004 - \frac{1.652}{d_p} - 1.547 \times 10^{-4}\left(d_p r\right)^2 - 0.21261 \log\left(d_p r\right)\right] + 1.652 r\left(1 - \frac{1}{K_{SR}}\right) \tag{24}$$

HP: power transmitted using the belt (hp). dp: pitch diameter of smaller pulley (in). r: Angular speed of smaller pulley (drive pulley), (rpm/1000). K_{SR}: Speed correction coefficient.

The correction factor for the angle of contact (K_θ) is derived from the following formula (Budynas & Nisbett, 2011).

$$\frac{D_d - d_d}{C} \tag{25}$$

D_p: Pitch diameter of large pulley (m). d_p: pitch diameter of the small pulley (m). C: The distance between the two centers of the pulleys (in).

Calculation of Modified Power (Budynas & Nisbett, 2011):

$$P_m = K_L \times K_\theta \times HP \tag{26}$$

P_m: modified power (hp). HP: Power transmitted using the belt (hp).: K_L: Belt length correction factor. K_θ: contact angle correction factor.

Determining the number of belt rows (Budynas & Nisbett, 2011):

$$N = \frac{P_T}{P_m} \tag{27}$$

N: number of belts. P_m: modified power (hp). P_T: input power to the smaller pulley (hp).

Transmission of power with a belt from pulley number 7 to 12 to the upper flat belt, two rows of belts are needed to transmit power in this direction. Power transmission from pulley numbers 11 to 14 to the upper flat belt has one path.

Chassis

The chassis is one of the main parts of any car. The main and necessary parts for each device are installed on the chassis. On the chassis of the peeling machine, the mentioned parts are placed (engine, power transmission system, peeling mechanism, etc.). A chassis can be a simple or complex framework. In the design of complex chassis, the installation location of the parts is precisely embedded.

The chassis is designed from a profile with a cross-section of 4 x 4 square centimeters and a thickness of 2 mm. In this chassis, the location of parts such as bearings, electric motor, power transmission system, blower fan, feeding tank and outlet opening are installed.

Figure 5. The right side is a view of the chassis design and the left side is a picture of the chassis.

De-Husking System

In this design, the movement of two conveyor belts with different speed and direction is used for peeling. The upper and lower conveyor belts are flat and have a small distance of about 2 mm. This distance is based on the average value of the width and thickness of six varieties of oats so that the distance value is slightly less than the thickness of the oat grains with the skin. The lower conveyor belt has a lower speed than the upper conveyor belt so this difference in speed and the faster movement of the upper conveyor belt causes rolling motion. The length of the lower conveyor belt is longer than the upper one, and the opening of the grain outlet tank is placed on it before the upper conveyor belt, so the grains are poured on it and it moves forward, and the upper conveyor belt, while having a higher speed, causes movement by moving on the grains. The grain is rotated and while the grain is between the two conveyor belts, it is slightly under pressure, and due to this pressure and the rotational movement, the skin is broken and separated from the grain. To prevent the lower belt from bending due to the pressure from the upper belt, a flat tray is installed under the lower belt.

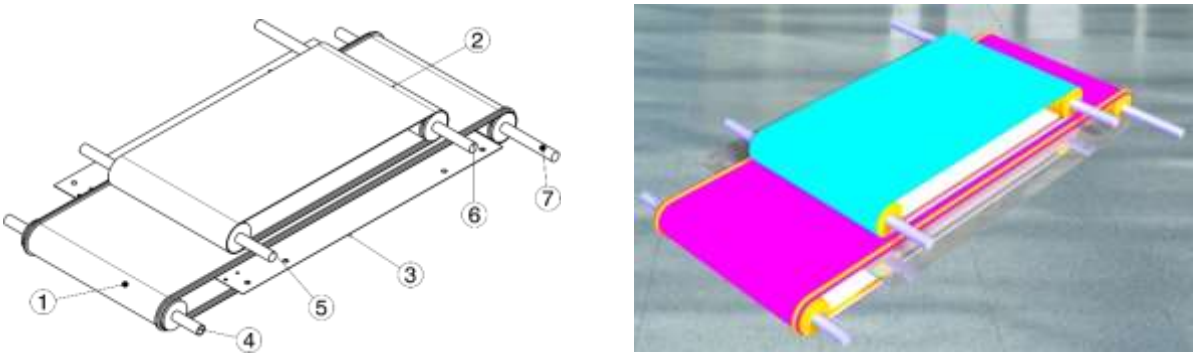

Figure 6. is a view of the de-husking mechanism; The right side of the diagram in the Ketia software, the left side of the de-husking system schematic: 1- lower flat belt, 2- upper flat belt, 3- metal tray, 4, 5- front moving roller of the belts, 6, 7- belt driving roller.

Result of calculation of the amount of peeled seeds

The amount of peeled grain is calculated based on the speed of the lower belt and the amount of grain exiting the tank every minute. The speed of the belt is 31.4 m/min and the length of the outlet opening of the tank is 248 mm. The distance between the outlet opening of the tank and the lower conveyor belt is adjusted so that the seeds are placed in a row on the conveyor belt. Therefore, the amount of grain output from the tank is obtained by the length and width of the oat

grain, the speed of the lower conveyor belt, and the length of the outlet mouth of the tank. The working method is to assume the length and width of the grains on the surface of the belt as a small rectangle, and the amount of output from the tank is calculated by considering the number of these rectangles, that is, by multiplying the length of the opening of the tank by the distance traveled by the lower conveyor belt. The amount of surface covered by the grain is obtained. This number is divided by the area of the oat seed and the number of seeds that are removed from the tank in one minute or one hour is calculated. By multiplying the number of grains by the average weight of six figures, the amount of peeled oats is 486 kg per hour, about half a ton.

Figure 7. The right side is a view of the original design and the left side is an image of the manufactured device.

Table 3. Physical characteristics of oat de-husking machine.

Device specifications	
Density	7860 kg/m^3
Volume	31260 cm^3
Mass	143 kg
Surface	108466 cm^2
Dimensions	1316×1362×620 mm
Center of gravity	X=5710.477 mm
	Y=-1652.342 mm
	Z=-4224.127 mm

Device evaluation

Machines always need to be analyzed during design and after construction. In this research, the efficiency of the device was determined using the percentage of peeled seeds. For the analysis, the amount of peeled seeds in a rectangular cube with dimensions of 10*10*15 cm was used and this test was done once for each cultivar due to limitations.

Evaluation results of peeled oats

As mentioned, the device was analyzed based on the amount of grains in the volume of 10*10*15 cubic centimeters. It took 5 seconds for the seeds to pass from the tank to the outlet.

Table 4. The results of the oat de-husking machine (results in percentage).

	Azarark	Brochure	Euro	Kowal	Putoro	Tarahumara
Healthy	68	58	24	40	42	**50**
Skinless	32	42	**76**	60	58	**50**

In the evaluation of the peeling machine, 76% of Euro varieties have been obtained.

REFRENCES

Amiss, J. M., Jones, F. D., Ryffel, H. H., McCauley, C. J., & Heald, R. (2004). *Guide to the Use of Tables and Formulas in*

Machinery's Handbook (27th Edition ed.). Industrial Press Inc.

Asli-Ardeh, E. A., Taghizadeh, G., & Taginezhad, E. (2022). Investigating the Effect of Some Operating Factors on the Performance of a Laboratory Cluster Threshing Machine–Case Study: Two Barley Varieties. *Biomechanism and Bioenergy Research*, *1*(2), 86-92. https://doi.org/10.22103/bbr.2022.20487.1035

Avallone, E., Baumeister, T., & Sadegh, A. (2006). *Marks' Standard Handbook for Mechanical Engineers. 10*. Citeseer.

Babeski, C. M., da Silva, J. A. G., Carvalho, I. R., Kraisig, A. R., da Rosa, J. A., Peter, C. L., . . . Schünemann, L. L. (2023). Agronomic Biofortification with Iron and Zinc on Yield and Quality of Oat Grains for the Validation of a Potential Resource for Nutritional Security. *Revista de Gestão Social e Ambiental*, *17*(8), e03924-e03924. https://doi.org/10.24857/rgsa.v17n8-020

Budynas, R. G., & Nisbett, J. K. (2011). *Shigley's mechanical engineering design* (Vol. 9). McGraw-Hill New York.

Doehlert, D. C. (2002). Quality improvement in oat. *Journal of crop production*, *5*(1-2), 165-189. https://doi.org/10.1300/J144v05n01_07

Khodabakhshian, R., Bayati, M., Shakeri, M., & Khojastepour, M. (2010). Design and manufacture of a pistachio peeling machine. *World Applied Sciences Journal*, *11*(8), 930-937.

Mirmoghtadaie, L., & Kadivar, M. (2013). Chemical modification of oat flour starch and protein and assessment of the physical characterisrics of a cake prepared using them. *Iranian Journal of Nutrition Sciences and Food Technology*, *8*(2), 103-113. (In Persian)

Rostami, M. A. (2008). Design, construction, and evaluation of a peanut peeler. *Agricultural engineering research*, *9*(1), 1-14. (In Persian)

Yang, Z., Xie, C., Bao, Y., Liu, F., Wang, H., & Wang, Y. (2023). Oat: Current state and challenges in plant-based food applications. *Trends in Food Science & Technology*, *134*, 56-71. https://doi.org/10.1016/j.tifs.2023.02.017